

Multi-objective optimization of slotted stator switched reluctance motor for electric vehicle application

Saif Kh Al-Farhan, Omar Sh Al-Yozbak

Department of of Electrical Engineering, College of Engineering, University of Mosul, Mosul, Iraq

Article Info

Article history:

Received Mar 23, 2023

Revised Apr 25, 2023

Accepted May 6, 2023

Keywords:

Genetic algorithm

Multi-objective optimization

Slot width/depth

Slotted stator teeth

Stator/rotor pole arc

Switched reluctance motors

ABSTRACT

The popularity of electric vehicles (EVs) and hybrid electric vehicles (HEVs) is projected to increase as environmental consciousness rises. They have emerged as a potential substitute for traditional electrical machines like the switched reluctance motors (SRMs). SRMs are renowned for their low cost of production and maintenance, built-in fault tolerance, and simple design. Additionally, because the machine's rotor construction does not require copper coils or permanent magnets, production costs are significantly reduced. However, it has disadvantages, including as high non-linearity, high torque ripple, and acoustic noise production. In this research, a method for designing slotted stator teeth switched reluctance motors (SST-SRM) in EVs using a genetic algorithm (GA) optimization design with multiple targets is provided. In order to achieve the best possible balance between peak torque (T_p), average torque (T_{avg}), and efficiency, the developed optimization function is chosen. The stator/rotor pole arc angle and slot width/depth are chosen as the optimized variables. When compared to traditional SRM, the optimization results of proposed SST-SRM demonstrate improvements in peak torque (24.40%, 36.98%, 42.73%, and 42.45%), average torque (7.40%, 29.94%, 33.00%, and 33.62%), and efficiency (0.27%, 0.52%, 0.97%, and 1.03%).

This is an open access article under the [CC BY-SA](https://creativecommons.org/licenses/by-sa/4.0/) license.



Corresponding Author:

Omar Sh Al-Yozbak

Department of Electrical Engineering, College of Engineering, University of Mosul

Mosul, Nineveh, Iraq

Email: o.yehya@uomosul.edu.iq

1. INTRODUCTION

Large-scale efforts to electrify transportation have been made recently in response to mounting concerns over fossil fuels and climate change. A significant number of people have recently developed an interest in electric vehicles (EVs) and hybrid electric vehicles (HEVs). The main ingredient of EVs is an electric motor, and several studies have been conducted to clearly appreciate them. For researchers, ensuring the steady operation of the electric motor through fault diagnosis is more complex and difficult [1]. Due to their high efficiency and excellent power density, permanent magnet synchronous motors (PMSMs) are widely employed in EVs technology [2]–[4]. Rare-earth elements are frequently used to make permanent magnets, although they have a number of disadvantages, such as being expensive and irreversibly demagnetizing at high temperatures. When trying to extract or remove rare-earth materials, additional environmental problems occur [5]. In recent years, there has been a lot of emphasis placed on the development of improved electric motors that are independent of rare-earth magnets [6]–[9], which are gaining in popularity. Switched reluctance motors (SRMs) have a number of benefits, including the absence of the need for rare earths. The SRM rotor's construction is simple and robust, and electrical steel is employed. SRMs also offer low maintenance and production costs. Inherently fault tolerant. The stator slots of the machine feature concentrated windings. Along

with these features, SRM has a wide range of speed and temperature capabilities [5]. The switched reluctance machine's advantage of variable speed operation [10]–[13], likewise, hostile environments. SRM research has a specific focus on EVs applications, which is attracting increasing interest from the research community [14]–[17]. The structure of SRMs, however, is consisted of doubly salient poles, which poses difficulties like high torque ripples, vibrations and high acoustic noise [18]. Vibrations and acoustic noise are mostly brought on by significant radial and axial forces for the configurations of axial and radial SRMs, respectively [19], [20]. Furthermore, thin air gaps between the rotor and stator, which distinguish SRMs and call for exact manufacturing accuracy [21]. Another flaw in the machine drive system is the requirement for unusual converters [21], [22].

In order to improve the machine's dynamic and static performance, these issues must be addressed, extensive study was conducted [23]. It is crucial to do study on how design parameters and current control affect electric motor performance in to develop methods for improving it. In addition, non-sinusoidal power supply cause harmonics that affect the performance of the motor, as it is necessary to reduce them to improve the dynamic performance of the electric motor [24]. To improve the performance of the machine, fresh configurations are created and optimization techniques are used. In order to overcome these drawbacks and compete with PMSMs, SRMs use topology optimization. In the previous literatures, in [25], the multi-objective Jaya approach is utilized to optimize the SRM design (MO-Jaya). In the Jaya algorithm, a solution is shifted from the poorest choice to the best one. The search has been greatly improved as a result. Additionally, the parameters are changed at random, producing a variety of outcomes. This study also advises against altering the best and worse options at random. The results demonstrate that there is more variety as a result. The MO-Jaya method was used to optimize the SRM for 8/6 and 6/4. The three main objectives are economy, iron weight and average torque.

Diao *et al.* [26] offers a distinctive multi-objective optimization design method for a SRM for low-speed electric automobiles. According to the findings, the SRM's performance must be maximized by optimizing six design characteristics, including acceleration time (including both overtaking time for acceleration and in situ acceleration time), maximum speed, maximum climbing gradient, torque ripple factor, climbing gradient, and energy use ratio. The key traits of low-speed EVs serve as the foundation for the driving motor's rated specifications. The SRM's dimensions within the designated parameter range have been verified to be valid using the engineering design technique. The vehicle balancing equation and the finite element model of the SRM were used to develop a dynamic simulation model in MATLAB/Simulink for a low-speed pure EVs propulsion system. The Taguchi-chicken swarm optimization method is then used to enhance the geometric parameters of the SRM for a number of objectives. The outcomes of the dynamic simulation and the testing of low speed EVs provide proof that the multi-objective optimization was accurate. The majority of research focuses on changing the magnetic flux distribution and reducing core losses, which are thought to be important factors that can affect how well various electrical appliances behave [27]. The slotted stator teeth switching reluctance motor (8/6 SST-SRM-5 kW) multi-objective design optimization is proposed in this research as a comprehensive framework. To maximize torque and efficiency of stator teeth switched reluctance motors (SST-SRM), the genetic algorithm (GA) is introduced. It is employed with variables of slot width/depth, stator/rotor pole arc, and multi-objective robust optimization technique. Following is the remainder of the essay. Section 2 included information on the operation and development of traditional SRM and proposed SST-SRM. Section 3 presented a multi-objective optimization model of the proposed SST-SRM. Results and implementation were provided in section 4. In section 5, the conclusion is drawn.

2. CONSTRUCTION OF SWITCHED RELUCTANCE MOTOR

A thorough knowledge of the mechanical structure of electrical machines is necessary for analysis and simulation. To get the appropriate output characteristics in various application, one must understand the electromagnetic behavior of each electric motor. In this section, the construction and principle working of the traditional SRM, and proposed SST-SRM are illustrated.

2.1. Principle working of traditional switched reluctance motor

A variable reluctance stepper motor with an efficient energy conversion system is the SRM. The SRM has a very simple design, as seen in Figure 1, with a brushless rotor and no windings of any type. The rotor and stator are both formed of laminated iron, and the motor is solely activated by the stator windings, which are concentric coils wrapped in series on diagonally opposing stator poles. Despite the motor's relatively simple form, a precise study of the SRM is exceedingly challenging and demanding because to the highly saturated operating situation and the motor's double salient structure. The tendency of the rotor to align with the excited stator pole in SRMs produces the electromagnetic torque by minimizing the reluctance (maximizing the inductance) of the magnetic path [28].

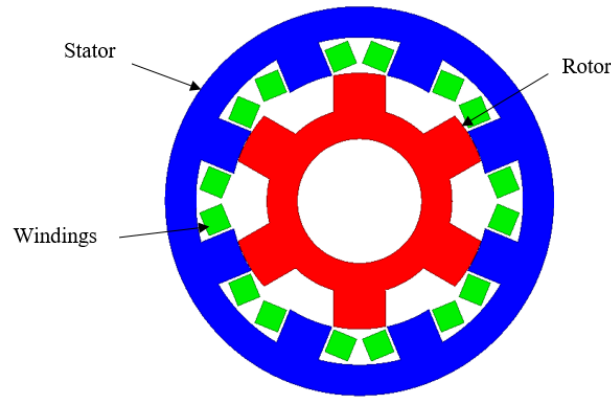


Figure 1. The traditional switched reluctance motor's construction

2.2. The proposed SRM

Figure 2 depicts the rotor and stator core cross-section of the proposed SST-SRM. The proposed model makes use of the slotted stator teeth to reduce the cost and core material usage. The correct stator core requirements must be employed in its production, including the diameter, kind of poles, slotted stator teeth, number of poles, and stack length of the core. The stator is made of iron because it has a high permeability and allows the flux to pass through it easily. The stator and rotor poles outer surface orientation, which determines the magnetic flux path, has a significant impact on the torque of the SRM.

As illustrated in Figure 3, by splitting the stator pole so that the symmetry of the newly formed two poles should remain the same, a portion of core material is removed for the design operation to make the 16/6 stator/rotor poles. Every stator pole gets a slot with a specific depth (h_d) and width (h_w). The rotor design resembles that of the traditional SRM's rotor. The requirements for the stator core design apply equally to the rotor core design.

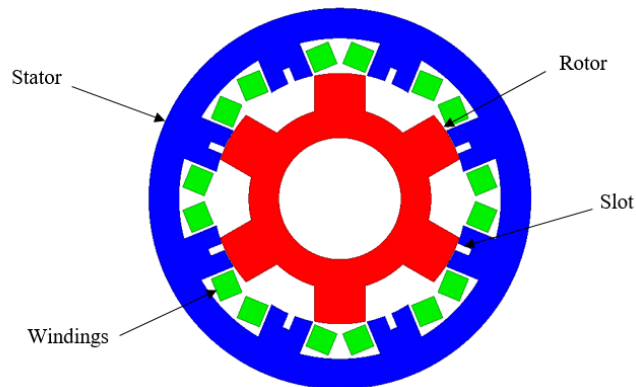


Figure 2. Cross-section of the SST-SRM model that has been proposed

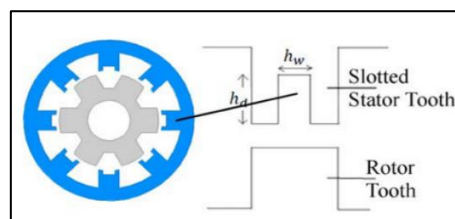


Figure 3. Slot characteristics [29]

3. THE PROPOSED SST-SRM MULTI-OBJECTIVE OPTIMIZATION MODEL

The proposed SST-SRM is built utilizing finite element analysis (FEA) and ansys electronics desktop simulation tools to execute the simulation. The variables and objective functions of the optimization technique used were determined with mechanical design considerations for the proposed SST-SRM. The parameters assigned to the motor's values are divided into model, study properties, materials, analysis conditions, circuit, and mesh generation once the motor has been built.

3.1. Optimization algorithms

The best solutions in the multi-objective optimization approach are essentially a compromise between all the goals. Algorithms for optimization are typically used to find the GA solutions. The multi-objective optimization issues have been subjected to a variety of optimization strategies. The genetic algorithm optimization is employed in this work. A potent stochastic technique for global search and optimization is the GA. When used to solve issues for which little prior knowledge of general topology is accessible, it is especially effective. This approach reaches a global optimum asymptotically and probabilistically. Thus, genetic algorithms imitate the biological process of evolution. Only those candidates with high fitness values are used to develop more solutions via crossover and mutation procedures after the solutions are evaluated according to a fitness value. Due to this method's efficiency and excellent convergence features, it has been used in many different domains of numeric programming. Although GA greatly simplifies these processes, it is nonetheless widely recognized as a useful tool for obtaining the best optimization results for a number of issues that are challenging to address using conventional mathematical (or) deterministic techniques [30]. The following are the main characteristics of GA optimization:

- a) Due to GA's stochastic character, there is a very high likelihood that the global optimal solution will be found.
- b) It is not essential to compute the objective function's gradient, which is required for the newton method, quasi-newton method, and gradient technique.
- c) Multivariable issues are simply handled, and the algorithm is significantly simpler to use.

As a result, the objectives of this study's design parameters are to maximize torque and efficiency. These variables include slot width/depth and stator/rotor pole arc. So far, no valid relational variations have been described. They are all inherently nonlinear. This forces us to employ any optimization strategies. If we choose appropriate values for the higher and lower variables limits and the maximum number of iterations, global optimization in GA is quite high. The traditional SRMs initial design parameters are displayed in Table 1.

Table 1. SRM first design criteria

Parameters	Value	Unit
Outside diameter of a stator	176.4	mm
Inner diameter of a stator	116.8	mm
Back iron thickness of a stator	13.8	mm
Air-gap size	0.35	mm
outside diameter of a rotor	116.1	mm
Stator/rotor poles	8/6	
Stator/rotor pole arc	20.2/23.5	deg
Stator/rotor pole height	16/16	mm
Number of turns/pole	75	
Slot fill factor	0.9	mm
The coil's height	9.6	mm
Stack length	171	mm
Stator/rotor core material	M19 steel	
Rated power	5	kW
Rated speed	3,000	rpm

3.2. Design variable consideration

The coil height and the stator pole height are practically similar. To ensure that the coils can be held in position, space should be given at the stator pole's tip for the pole shoes and wedges [28]. Therefore, the slot depth is equal to the stator pole height and slot width is equal to pole face length. To produce a unidirectional torque, the poles of the excited stator phase and the poles of the rotor must overlap. Otherwise, there would be "gaps" when no torque is generated (the overlap angle should be higher than the step angle). Furthermore, to give the largest practical variation of phase inductance with rotor position, the rotor's inter-polar arc must be bigger than the stator pole arc. The fact that the stator pole is typically intended to be a little bit smaller than the rotor pole arc places further restrictions on the pole arcs [31]. As a result, it is possible to slightly improve the slot area, copper winding cross section, and aligned/unaligned inductance ratio. The restrictions are set

using the feasible triangle's guidelines [31], it specifies the range of combinations that are often acceptable. Of course, the performance of SRM as described by the various points of this triangle varies significantly. However, this is dependent on a number of variables, including torque ripple, starting torque, and saturation's impact. To maximize peak torque, average torque, and efficiency, on the one hand. The limitations, which are specified as, should restrict the slot's width/ depth, and stator/rotor pole arc angle as shown in (1)-(6) [28]:

$$0.5 \leq h_w \leq 18 \tag{1}$$

$$1 \leq h_d \leq 16 \tag{2}$$

$$0.3333 \leq \frac{\beta_s}{\theta_{sp}} \leq 0.5555 \tag{3}$$

$$0.25 \leq \frac{\beta_r}{\theta_{rp}} \leq 0.5 \tag{4}$$

$$\theta_{sp} = \frac{360}{N_s} \tag{5}$$

$$\theta_{rp} = \frac{360}{N_r} \tag{6}$$

where h_w is slot width, h_d is slot depth, N_s is the number of stator poles, N_r is the number of rotor poles, θ_{sp} and, θ_{rp} are respectively the stator pole pitch angle and the rotor pole pitch angle. Contrasted with, the peak current for torque generation is produced by the inductance in the completely aligned position. Additionally, the ratio of the rotor to stator pole arc angles affects the fully aligned inductance. As long as the perfectly aligned inductance value can only vary by 15% and the self-starting requirement is taken into account, the ratio of the rotor pole arc angle to the stator pole arc angle should be kept within the range by (7) [28]:

$$1.0 \leq \frac{\beta_r}{\beta_s} \leq 2 \tag{7}$$

because self-starting is necessary, calculated as follows is the minimum stator pole arc angle by (8) [28]:

$$\beta_s \geq \frac{720}{N_s N_r} \tag{8}$$

the optimization of the stator/rotor pole arc angle and slot width/depth must be constrained by (1)-(8).

4. IMPLEMENTATION AND RESULTS

The proposed (SST-SRM 16/6) model and the traditional (SRM 8/6) model are both subject to the design procedure. A collection of outputs of magnetic flux vector plots and graphs with varied features have been obtained after the analysis for both designs has been completed. In adding, the traditional and proposed SST-SRM torque graphs are compared and verified.

4.1. The traditional SRM

After the completion of finite element (FE) analysis for traditional SRM, by simulation the conventional motor at different speeds to obtain the output characteristics shown in the Table 2. Table 2 shows the values of peak torque, average torque and efficiency of a traditional motor when running at speeds (30%, 50%, 70%, and 100%) of rated speed. The torque has a higher value at low speeds and gradually decreases at the rated speed.

Table 2. Performance of traditional SRM

#	β_r (deg)	β_s (deg)	Speed (rpm)	Tp (N.m)	Tavg (N.m)	Efficiency
1			900	37.3548	17.7199	91.41839
2	23.5	20.2	1,500	18.1988	6.453	93.73743
3			2,250	9.1066	2.9005	93.59091
4			3,000	5.2508	1.7289	93.46123

Figure 4 displays the torque determined from FE analysis of traditional SRM. Figure 4(a) shows that the peak torque measured (37.3548 N.m) at speed (900 rpm). In Figure 4(b) the peak torque measured (18.1988 N.m) at speed (1,500 rpm). Therefore, Figure 4(c) the peak torque measured (9.1066 N.m) at speed (2,250 rpm). Additionally, Figure 4(d) the peak torque measured (5.2508 N.m) at speed (3,000 rpm).

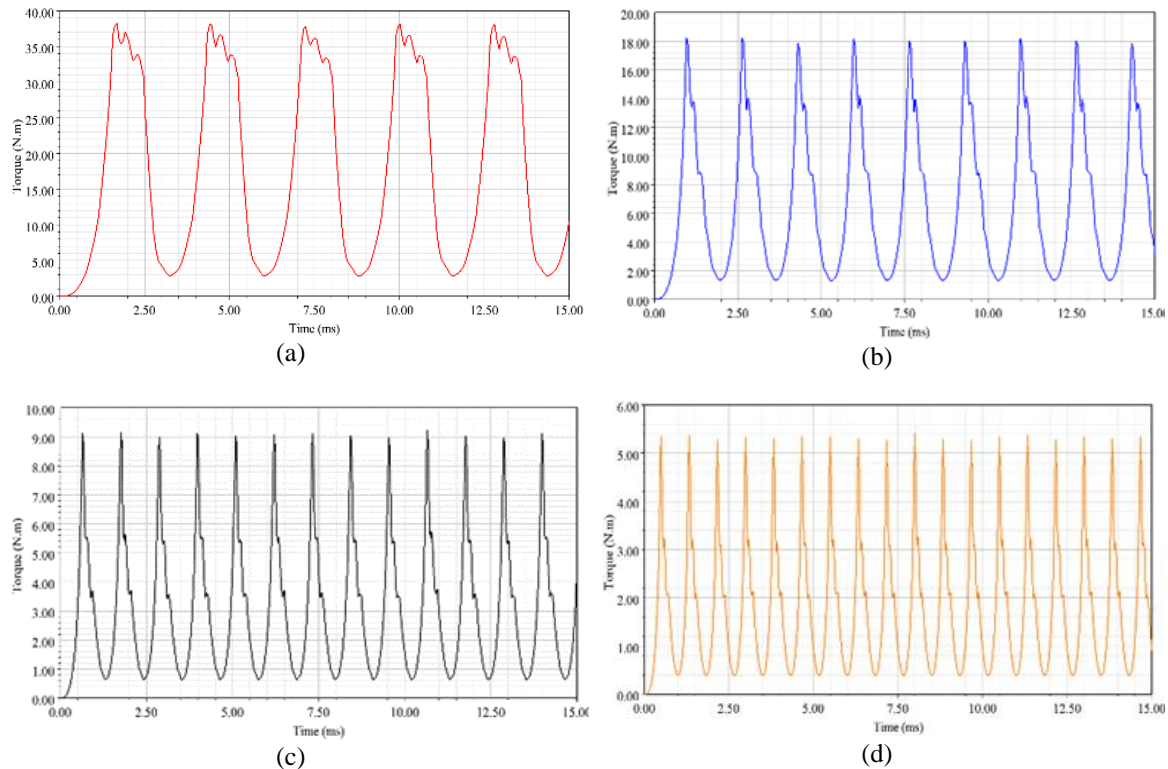


Figure 4. Torque of the traditional SRM for (a) speed=900 rpm, (b) speed=1,500 rpm, (c) speed=2,250 rpm, and (d) speed=3,000 rpm

4.2. The proposed SST-SRM

In the proposed SST-SRM, the only adjustments are made with slot width/depth and stator/rotor pole arc by GA multi-objective optimization and how many stator poles have slotted teeth. The slotted stator teeth's finite element analysis SST-SRM has been carried out using the same set of parameters as the traditional SRM, and stator poles with the 16/6 model of SRM show output values that fluctuate in relation to the torque and flux linkage. Figures 5 and 6 displays the magnetic flux density's vector plot for the proposed SST-SRM at speeds of (30%, 50%, 70%, and 100%) of rated speed under alignment and non-alignment conditions respectively. This graphics shows the variation in magnetic flux densities, with the corner of the stator and rotor tooth showing the highest flux density value. When its operating principle is accepted, the behavior of the magnetic field lines changes dramatically. As the width of the poles narrows, concentration of the magnetic field lines increases, raising the saturation value range. Figures 5(a)-5(d) shows that the proposed SST-SRM model performs better and produces better magnetic flux distribution results than the traditional one at speeds of (30%, 50%, 70%, and 100%) of rated speed under alignment condition which reluctance is minimum and inductance is maximum, according to the FE study.

In addition, Figures 6(a)-6(d) shows that the proposed SST-SRM model performs better and produces better magnetic flux distribution results than the traditional one at speeds of (30%, 50%, 70%, and 100%) of rated speed under non-alignment condition which reluctance is maximum and inductance is minimum, according to the FE study. For the different values of slot width/depth and stator/rotor pole arc, the torque and efficiency values are also different.

After applying the multi-objective genetic algorithm optimization of the proposed SST-SRM, and by generating several values for the optimization technique variables. The cases that give the optimum values for the output characteristics of the proposed SST-SRM were selected. Table 3 shows the optimum values for torque and efficiency of the proposed SST-SRM compared with traditional SRM.

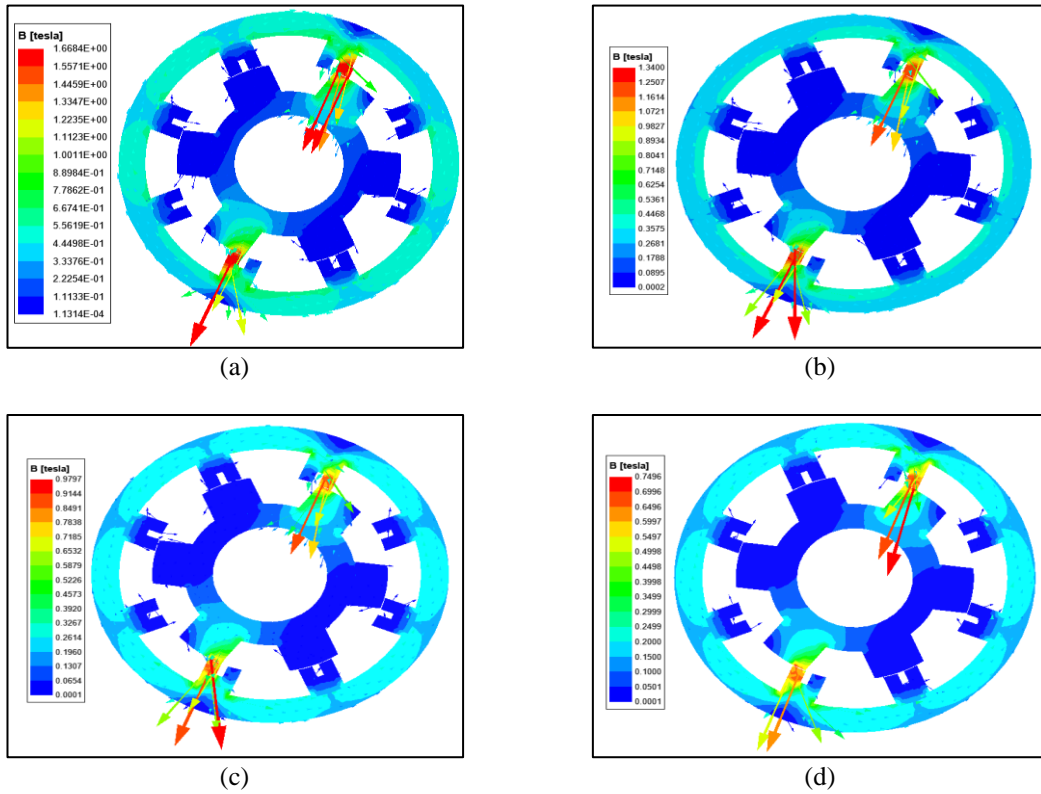


Figure 5. Magnetic flux vector plot of proposed SST-SRM under alignment condition for: (a) speed=900 rpm, (b) speed=1,500 rpm, (c) speed=2,250 rpm, and (d) speed=3,000 rpm

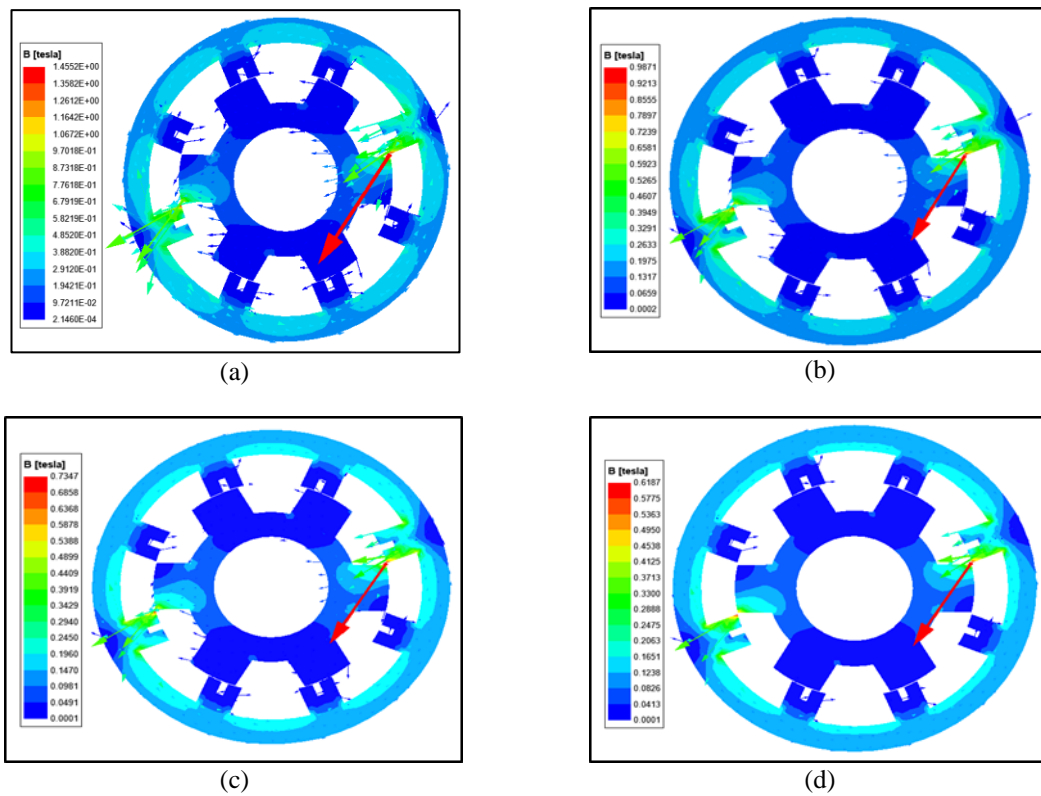


Figure 6. Magnetic flux vector plot of proposed SST-SRM under non-alignment condition for: (a) speed=900 rpm, (b) speed=1,500 rpm, (c) speed=2,250 rpm, and (d) speed=3,000 rpm

Table 3. Multi-objective optimization results of proposed SST-SRM

Speed (rpm)	Cases	h_w (mm)	h_d (mm)	β_r (deg)	β_s (deg)	Tp (N.m)	Tavg (N.m)	Efficiency
900	Case 1	0.961165197	4.002777184	26.17671438	17.32611515	40.34	18.533	90.87581477
	Case 2	3.46458327	6.842768639	25.55589465	18.99200342	45.3715	18.9273	90.93152572
	Case 3	3.481429487	7.346507157	25.6642964	17.42981991	46.4721	19.0327	91.66614034
	Case 4	4.3865627	8.623584704	22.82417066	17.13767176	45.1595	18.6667	89.75552266
1,500	Case 1	0.961165197	4.002777184	26.17671438	17.32611515	19.2694	7.4023	94.22925387
	Case 2	3.46458327	6.842768639	25.55589465	18.99200342	23.8938	8.2438	93.28423035
	Case 3	3.481429487	7.346507157	25.6642964	17.42981991	24.9289	8.3855	94.23348912
	Case 4	4.3865627	8.623584704	22.82417066	17.13767176	23.3403	7.7923	94.18557436
2,250	Case 1	0.961165197	4.002777184	26.17671438	17.32611515	9.4051	3.3586	94.25747047
	Case 2	3.46458327	6.842768639	25.55589465	18.99200342	12.1775	3.7737	94.44236391
	Case 3	3.481429487	7.346507157	25.6642964	17.42981991	12.9979	3.8578	94.49899523
	Case 4	4.3865627	8.623584704	22.82417066	17.13767176	12.0473	3.3372	93.29136886
3,000	Case 1	0.961165197	4.002777184	26.17671438	17.32611515	5.4965	1.9962	94.09153184
	Case 2	3.46458327	6.842768639	25.55589465	18.99200342	7.0984	2.2511	94.3500313
	Case 3	3.481429487	7.346507157	25.6642964	17.42981991	7.4802	2.3103	94.42544966
	Case 4	4.3865627	8.623584704	22.82417066	17.13767176	7.4555	1.952	93.16355665

In order to obtain the optimal values, from Table 3 at ($h_w=3.481429487$ mm, $h_d=7.346507157$ mm, $\beta_r=25.6642964^\circ$, $\beta_s=17.42981991^\circ$) it is shown that the peak torque increased with [9.11, 6.73, 3.89, 2.22 (N.m)], average torque increased with [1.31, 1.93, 0.95, 0.58 (N.m)] for speeds [900, 1,500, 2,250, 3,000 (rpm)] respectively. At same optimum values of ($h_w, h_d, \beta_r, \beta_s$) the efficiency increased with [0.24, 0.49, 0.9, 0.96] for speeds [900, 1,500, 2,250, 3,000 (rpm)] respectively. Figure 7 displays the proposed SST-SRM's torque characteristics. From the graph in Figure 7(a), at speed=900 rpm, the optimum values of $T_p=46.4721$ N.m, $T_{avg}=19.0327$ N.m, and efficiency=91.66614034 have been occurred at ($h_w=3.481429487$ mm, $h_d=7.346507157$ mm, $\beta_r=25.6642964^\circ$, $\beta_s=17.42981991^\circ$).

While the graph in Figure 7(b), at speed=1,500 rpm, the optimum values of $T_p=24.9289$ N.m, $T_{avg}=8.3855$ N.m, and efficiency=94.23348912 have been occurred at ($h_w=3.481429487$ mm, $h_d=7.346507157$ mm, $\beta_r=25.6642964^\circ$, $\beta_s=17.42981991^\circ$). Therefore, the graph in Figure 7(c), at speed=2,250 rpm, the optimum values of $T_p=12.9979$ N.m, $T_{avg}=3.8578$ N.m, and efficiency=94.49899523 have been occurred at ($h_w=3.481429487$ mm, $h_d=7.346507157$ mm, $\beta_r=25.6642964^\circ$, $\beta_s=17.42981991^\circ$). Additionally, the graph in Figure 7(d), at 3,000 rpm, the optimum values of $T_p=7.4802$ N.m, $T_{avg}=2.3103$ N.m, and efficiency=94.42544966 have been occurred at ($h_w=3.481429487$ mm, $h_d=7.346507157$ mm, $\beta_r=25.6642964^\circ$, $\beta_s=17.42981991^\circ$).

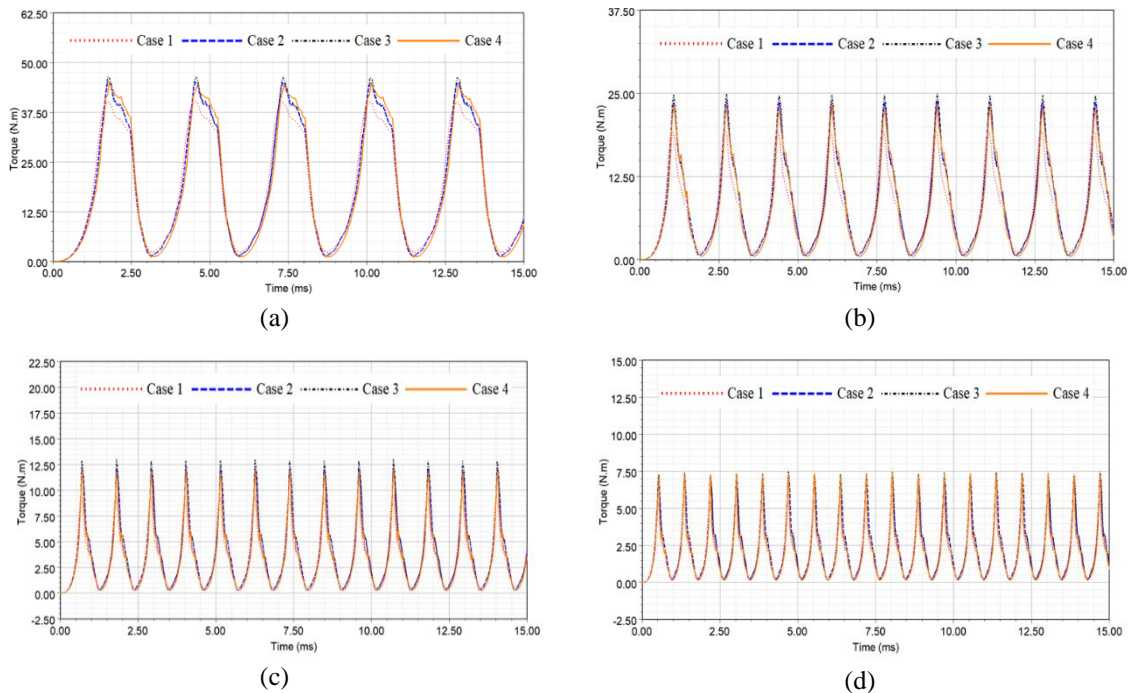


Figure 7. Optimal torque of the proposed SST-SRM for speeds for (a) speed=900 rpm, (b) speed=1,500 rpm, (c) speed=2,250 rpm, and (d) speed=3,000 rpm

The evaluation between traditional SRM and optimum proposed SST-SRM results for peak/average torque and efficiency shown in Figure 8. For Figure 8(a) shows, the optimum value of peak torque for the proposed SST-SRM compared with traditional model for speeds (900, 1,500, 2,250, and 3,000) rpm. In Figure 8(b) shows, the optimum value of average torque for the proposed SST-SRM compared with traditional model for speeds (900, 1,500, 2,250, and 3,000) rpm. As well as in Figure 8(c) shows, the optimum value of efficiency for the proposed SST-SRM compared with traditional model for speeds (900, 1,500, 2,250, and 3,000) rpm. Despite the increase in torque, the materials mass, volume, and weight are all reduced, which undoubtedly lowers the cost. Table 4 compares the proposed and traditional models for the material with the same mass density of Iron 7267.5 (gm/cm³) (h w=3.481429487 mm, h d=7.346507157 mm, $\beta_r=25.6642964$, $\beta_s=17.42981991$).

According to Table 4, the proposed SST-SRM has a reduced mass of approximately 0.24 kg, or around 2% of the total mass of the traditional SRM. Although the stator core material was reduced by adding slots, the output characteristics of the proposed SST-SRM were improved. Reducing the cost of the proposed SST-SRM reduces the total cost of EVs and makes them competitive with traditional vehicle that internal combustion engines.

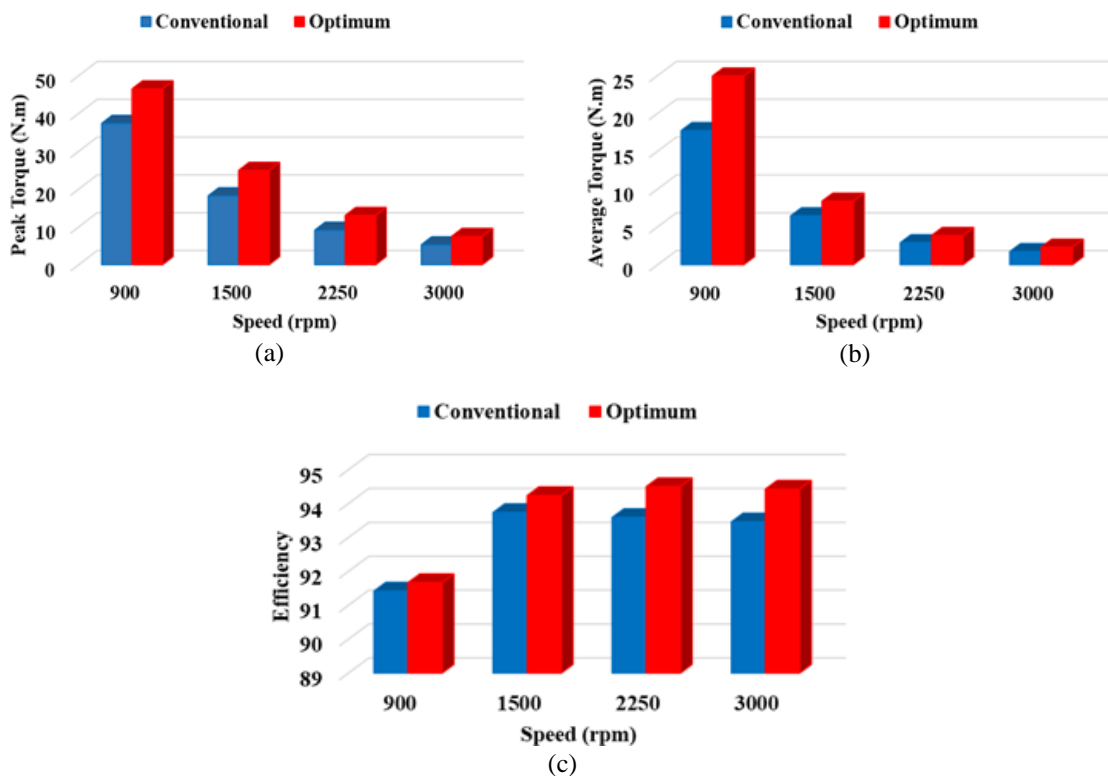


Figure 8. The Evaluation between traditional SRM and optimal values results of the proposed SST-SRM for (a) peak torque, (b) average torque, and (c) efficiency

Table 4. Mass comparison of the best-proposed SST-SRM and the traditional SRM

Design topology	Volume (mm ³)	Mass (kg)
Traditional SRM	1,655,603.46	12.03
Proposed SST-SRM	1,622,955.12	11.79

5. CONCLUSION

In this study, a new SST-SRM design proposal is presented, and an analysis using a FE analysis tool has been done for the application to an electric vehicle. In order to improve the torque and efficiency values, a method for GA multi-objective design optimization has been implemented. The stator/rotor pole arc and slotted stator teeth of the stator poles to a specific slot width/depth make up the new proposed design. When compared to the traditional SRM, the novel slotted stator tooth stator pole (16/6) design exhibits a large range of torque magnitude variation for improvements in peak torque of around (24.40%, 36.98%, 42.73%, and 42.45%).

Additionally, it displays large range of variations in torque magnitude for improvements in average torque of approximately (7.40%, 29.94%, 33.00%, and 33.62%) as well as variance efficiency magnitude with improvements of around (0.27%, 0.52%, 0.97%, and 1.03%). Additionally, an estimated 2% less stator core material has been used, which makes it both affordable and lightweight for the same rated output. For its use in electric car applications, the suggested SRM model exhibits strong vibrancy and improvements in the output parameters.

ACKNOWLEDGEMENTS

Authors would like to thank Mosul University, College of Engineering, Electrical Department, for the support given during this work.





REFERENCES

- [1] O. S. Alyozbaky and M. A. Al-Yoonus, "Faults diagnosis of a single-phase induction motor using microcontroller," *International Journal of Advanced Science and Technology*, vol. 29, no. 3, pp. 4866–4875, 2020.
- [2] J. O. Estima and A. J. M. Cardoso, "Efficiency analysis of drive train topologies applied to electric/hybrid vehicles," *IEEE Transactions on Vehicular Technology*, vol. 61, no. 3, pp. 1021–1031, 2012, doi: 10.1109/TVT.2012.2186993.
- [3] X. Liu, H. Chen, J. Zhao, and A. Belahcen, "Research on the performances and parameters of interior PMSM used for electric vehicles," *IEEE Transactions on Industrial Electronics*, vol. 63, no. 6, pp. 3533–3545, 2016, doi: 10.1109/TIE.2016.2524415.
- [4] Z. Xia *et al.*, "Computation-efficient online optimal tracking method for permanent magnet synchronous machine drives for MTPA and flux-weakening operations," *IEEE Journal of Emerging and Selected Topics in Power Electronics*, vol. 9, no. 5, pp. 5341–5353, 2021, doi: 10.1109/JESTPE.2020.3039205.
- [5] D. Xiao *et al.*, "Universal full-speed sensorless control scheme for interior permanent magnet synchronous motors," *IEEE Transactions on Power Electronics*, vol. 36, no. 4, pp. 4723–4737, 2021, doi: 10.1109/TPEL.2020.3023140.
- [6] B. Bilgin, J. W. Jiang, and A. Emadi, "Switched reluctance motor drives fundamentals to applications," Boca Raton, Florida: CRC Press LLC, 2018.
- [7] K. Kiyota and A. Chiba, "Design of switched reluctance motor competitive to 60-kW IPMSM in third-generation hybrid electric vehicle," *IEEE Transactions on Industry Applications*, vol. 48, no. 6, pp. 2303–2309, 2012, doi: 10.1109/TIA.2012.2227091.
- [8] I. Boldea, L. N. Tutelea, L. Parsa, and D. Dorrell, "Automotive electric propulsion systems with reduced or no permanent magnets: an overview," *IEEE Transactions on Industrial Electronics*, vol. 61, no. 10, pp. 5696–5711, 2014, doi: 10.1109/TIE.2014.2301754.
- [9] F. P. Scalcon *et al.*, "Robust control of synchronous reluctance motors by means of linear matrix inequalities," *IEEE Transactions on Energy Conversion*, vol. 36, no. 2, pp. 779–788, 2021, doi: 10.1109/TEC.2020.3028568.
- [10] D. Xiao, J. Ye, G. Fang, Z. Xia, X. Wang, and A. Emadi, "Improved feature position based sensorless control scheme for SRM drives based on nonlinear state observer at medium and high speeds," *IEEE Transactions on Power Electronics*, vol. 36, no. 5, pp. 5711–5723, 2021, doi: 10.1109/TPEL.2020.3030007.
- [11] F. Peng, J. Ye, A. Emadi, and Y. Huang, "Position sensorless control of switched reluctance motor drives based on numerical method," *IEEE Transactions on Industry Applications*, vol. 53, no. 3, pp. 2159–2168, 2017, doi: 10.1109/TIA.2017.2672523.
- [12] J. B. Bartolo, M. Degano, J. Espina, and C. Gerada, "Design and initial testing of a high-speed 45-kW switched reluctance drive for aerospace application," *IEEE Transactions on Industrial Electronics*, vol. 64, no. 2, pp. 988–997, 2017, doi: 10.1109/TIE.2016.2618342.
- [13] T. A. D. S. Barros, P. J. D. S. Neto, P. S. N. Filho, A. B. Moreira, and E. R. Filho, "An approach for switched reluctance generator in a wind generation system with a wide range of operation speed," *IEEE Transactions on Power Electronics*, vol. 32, no. 11, pp. 8277–8292, 2017, doi: 10.1109/TPEL.2017.2697822.
- [14] J. Zhu, K. W. E. Cheng, and X. Xue, "Design and analysis of a new enhanced torque hybrid switched reluctance motor," *IEEE Transactions on Energy Conversion*, vol. 33, no. 4, pp. 1965–1977, 2018, doi: 10.1109/TEC.2018.2876306.
- [15] C. R. D. Osorio, F. P. Scalcon, R. P. Vieira, V. F. Montagner, and H. A. Grundling, "Robust control of switched reluctance generator in connection with a grid-tied inverter," *2019 IEEE 15th Brazilian Power Electronics Conference and 5th IEEE Southern Power Electronics Conference, COBEP/SPEC 2019*, 2019, pp. 8–13, doi: 10.1109/COBEP/SPEC44138.2019.9065551.
- [16] B. Howey, B. Bilgin, and A. Emadi, "Design of an external-rotor direct drive E-bike switched reluctance motor," *IEEE Transactions on Vehicular Technology*, vol. 69, no. 3, pp. 2552–2562, 2020, doi: 10.1109/TVT.2020.2965943.
- [17] L. Ge, B. Burkhart, and R. W. D. Doncker, "Fast iron loss and thermal prediction method for power density and efficiency improvement in switched reluctance machines," *IEEE Transactions on Industrial Electronics*, vol. 67, no. 6, pp. 4463–4473, 2020, doi: 10.1109/TIE.2019.2922937.
- [18] H. Zhang, W. Xu, S. Wang, Y. Huangfu, G. Wang, and J. Zhu, "Optimum design of rotor for high-speed switched reluctance motor using level set method," *IEEE Transactions on Magnetics*, vol. 50, no. 2, pp. 765–768, 2014, doi: 10.1109/TMAG.2013.2285393.
- [19] B. G. Joseph, "Variable reluctance axial flux alternator incorporating air gap variation," *In 2016 Biennial International Conference on Power and Energy Systems: Towards Sustainable Energy (PESTSE)*, 2016, pp. 1–8.
- [20] M. M. Nezamabadi, E. Afjei, and H. Torkaman, "Design, dynamic electromagnetic analysis, FEM, and fabrication of a new switched-reluctance motor with hybrid motion," *IEEE Transactions on Magnetics*, vol. 52, no. 4, 2016, doi: 10.1109/TMAG.2015.2504522.
- [21] N. K. Sheth and K. R. Rajagopal, "Effects of nonuniform airgap on the torque characteristics of a switched reluctance motor," *IEEE Transactions on Magnetics*, vol. 40, no. 4, pp. 2032–2034, 2004, doi: 10.1109/TMAG.2004.832173.
- [22] H. Torkaman and E. Afjei, "Sensorless method for eccentricity fault monitoring and diagnosis in switched reluctance machines based on stator voltage signature," *IEEE Transactions on Magnetics*, vol. 49, no. 2, pp. 912–920, 2013, doi: 10.1109/TMAG.2012.2213606.
- [23] N. Zabihi and R. Gouws, "A review on switched reluctance machines for electric vehicles," *IEEE International Symposium on Industrial Electronics*, vol. 2016-Novem, pp. 799–804, 2016, doi: 10.1109/ISIE.2016.7744992.
- [24] O. S. A. Alyozbaky and M. Z. A. Ab-Kadir, "Influence of non-sinusoidal power supply on the performance of a single-phase capacitor induction motor," *Indonesian Journal of Electrical Engineering and Computer Science (IJECS)*, vol. 25, no. 3, pp. 1246–1257, 2022, doi: 10.11591/ijeecs.v25.i3.pp1246-1257.





- [25] M. El-Nemr, M. Afifi, H. Rezk, and M. Ibrahim, "Finite element based overall optimization of switched reluctance motor using multi-objective genetic algorithm (Nsga-ii)," *Mathematics*, vol. 9, no. 5, pp. 1–20, 2021, doi: 10.3390/math9050576.
- [26] K. Diao, X. Sun, G. Lei, Y. Guo, and J. Zhu, "Multimode optimization of switched reluctance machines in hybrid electric vehicles," *IEEE Transactions on Energy Conversion*, vol. 36, no. 3, pp. 2217–2226, 2021, doi: 10.1109/TEC.2020.3046721.
- [27] M. M. Isa, M. Z. A. Ab-Kadir, C. Gomes, N. Azis, M. Izadi, and O. S. H. Alyozbaky, "Analysis on magnetic flux density and core loss for hexagonal and butt-lap core joint transformers," *2016 IEEE 2nd Annual Southern Power Electronics Conference, SPEC 2016*, 2016, pp. 7–10, doi: 10.1109/SPEC.2016.7846227.
- [28] R. Krishnan, "Switched reluctance motor drives : modeling, simulation, analysis, design, and application," CRC Press, 2017.
- [29] M. A. Patel *et al.*, "Design and optimisation of slotted stator tooth switched reluctance motor for torque enhancement for electric vehicle applications," *International Journal of Ambient Energy*, vol. 43, no. 1, pp. 4283–4288, 2021, doi: 10.1080/01430750.2021.1873857.
- [30] H. Singh, "Enhancement of switched reluctance motor system using optimization algorithms: a review and open research challenges," *Global Research and Development Journals*, vol. 7, no. 7, pp. 1–4, 2022.
- [31] N. R. Patel and J. K. Chavda, "Design and performance analysis of 8/6 radial field switched reluctance motor for electric vehicle application," *UGC Care Approved Journal*, vol. 26, no. 3, pp. 2013–2015, 2021.

BIOGRAPHIES OF AUTHORS



Saif Kh Al-Farhan     was born in Ninawa, Iraq, in 1991. He received his bachelor of science (B.Sc.) degree in electrical engineering from the electrical engineering department, college of engineering, University of Mosul, Iraq, in 2013. Then he was appointed assistant engineer at the Iraqi Ministry of Oil-State Company for gas filling and services, where his work focuses on the various electrical machines used in liquid gas filling plants. Where he is currently pursuing the M.Sc. degree. His main research interest includes optimization, SRM design and control for automobile application. He can be contacted at email: saif.21enp17@student.uomosul.edu.iq.



Omar Sh Al-Yozbaky     he obtained his bachelor of science (B.Sc.) in electrical engineering in 2001 from the electrical engineering department, college of engineering, University of Mosul, Iraq. Then he was appointed as an assistant engineer in the same mentioned department. After that, he got M.Sc. in "overcome the effect of critical distance in XLPE high voltage cables by inductive shunt compensator", in 2008 from the same mentioned department as well. Upon his graduation, he was appointed as teaching staff (assistant lecturer) in the electrical engineering department, college of engineering, University of Mosul. In 2012, he obtained the scientific title (lecturer) and the Ph.D. degree in the department of electrical and electronic engineering, faculty of engineering, University Putra Malaysia in 2017. Since 2014, he was a member of the Centre for Electromagnetic and lightning protection research (CELP). Now, he is assistant professor electrical engineering department, college of engineering, University of Mosul. The subjects for interest, renewable energy fields associated with the smart grid, thermal modeling transformer design, and electrical machines. He can be contacted at email: o.yehya@uomosul.edu.iq.